ELECTRICAL IMPEDANCE OF ISOLATED AMNION

GORDON A. SILVER, JOSÉ STRAUSS, *and* GEORGE A. MISRAHY

From the Developmental and Sensory Physiology Laboratory, Childrens Hospital of Los Angeles, Los Angeles. Dr. Silver's present address is the California State Polytechnic College, Physical Sciences Department, San Luis Obispo, California.

ABSTRACT The electrical impedance of the guinea pig amniotic membrane was measured, under standardized conditions, over the frequency range of 20 to 7000 cycles/second. This impedance can be represented analytically by a simple frequency-dependent function which is precisely of the *form* of the Debye relaxation equation. The observed data exhibit a broad dispersion centered at a frequency of 1050 cycles/second and a narrow distribution of time constants centered about 152 microseconds, both effects being due to the polydisperse nature of amniotic tissue. If the narrow time-constant distribution is approximated by a single time constant, amnion impedance can be simulated by a simple electrical circuit of frequency-independent elements. The Maxwell-Wagner interfacial treatment, although successfully adapted for cell suspensions, is shown to lose its quantitative significance in the case of the tightly structured amnion. In addition, determinations were made on the chemical composition of amniotic fluid, fetal blood and urine, and maternal blood and urine; the DC potential across the amniotic membrane was also measured.

INTRODUCTION

Electrical impedance of biological material is a function of frequency. Low frequency conductance is generally associated with ionic permeability while capacitance is related to polarization processes (1).

The present paper introduces a new preparation for the study of impedance in biological tissues, the guinea pig amnion. There are several unique properties of the amnion which make it especially suited for impedance measurements. Its size, accessibility, and ruggedness make it a convenient experimental preparation. Its avascularity allows repeated measurements to be made, free from the influence of hemodynamic changes. In addition, the amnion possesses a relatively simple geometry; two layers of evenly spaced cuboidal cells.

The present paper reports the electrical impedance over the audiofrequency range of the guinea pig amniotic membrane under standardized conditions. Mathematical relations appropriate to relaxation phenomena are employed to describe

the impedance data. Determinations were made of the chemical composition of amniotic fluid, fetal blood and urine, and maternal blood and urine; the DC potential across the amniotic membrane was also measured. These measurements are presented in the Appendix.

RELAXATION AND DISPERSION

In application of relaxation theory to biological materials (1) it has been found that a plot of resistance *vs.* reactance of the measured impedance ($Z = R + jX$) is a semicircle whose center lies above $X = 0$. Analytically such a function is represented by

$$Z = R_\infty + \frac{R_0 - R_\infty}{1 + (j\omega\tau)^{1-\alpha}} \tag{1}$$

where α is formally required to displace the center from the real axis (4) and may be defined by

$$\alpha = (2/\pi) \sin^{-1} (d/r) \tag{2}$$

where r is the radius of the circular arc and d is the distance of its center from the R axis. In question (1) the subscripts 0 and ∞ refer to zero and infinite frequencies, τ is the time constant, ω is the angular frequency, and j is the square root of -1. Note that if $\alpha = 0$ equation (1) is precisely of the *form* of the Debye relaxation equation (2, 3). The real and imaginary parts of equation (1) are:

$$R = R_\infty + \frac{(R_0 - R_\infty)[1 + (\omega\tau)^\beta \sin (\alpha\pi/2)]}{1 + 2(\omega\tau)^\beta \sin (\alpha\pi/2) + (\omega\tau)^{2\beta}} \tag{3}$$

$$X = -\frac{(R_0 - R_\infty)(\omega\tau)^\beta \cos (\alpha\pi/2)}{1 + 2(\omega\tau)^\beta \sin (\alpha\pi/2) + (\omega\tau)^{2\beta}} \tag{4}$$

where $\beta = 1 - \alpha$. If it is assumed that the relaxation is the result of a continuous distribution of time constants, equation (1) may be rewritten as

$$Z = R_\infty + (R_0 - R_\infty) \int_0^\infty \frac{f(\tau)\, d\tau}{1 + j\omega\tau} \tag{5}$$

where $f(\tau)$ is the distribution function. Fuoss and Kirkwood (5) developed an analytical method for determining $f(\tau)$ provided the data could be empirically represented by an integrable analytic function. Applying this technique to equation (1) Cole and Cole (4) find

$$f(s) = \frac{\sin (\alpha\pi)}{\cosh [(1 - \alpha)s] - \cos (\alpha\pi)} \tag{6}$$

where

$$s = \ln (\tau/\tau_0) \tag{7}$$

and τ_0 is the most probable time constant. In view of the empirical entry of the term α there is no *a priori* reason for regarding equation (6) as anything more than an empirical relation. Further, note that the distribution function, $f(\tau)$, as presented applies only in the impedance plane and that an admittance presentation would be differently weighted. Other distribution functions have been considered (6) but the Cole and Cole function of equation (6) is preferred because of its good agreement with experimental data and its analytical convenience.

PROCEDURE

Amniotic membranes were obtained from pregnant guinea pigs (weight: 815 to 1340 gm) under dial with urethane (Ciba, Inc., Summit, New Jersey) anesthesia (0.5 cc/kg). The uterus was exposed by an abdominal midline incision. The uterus was incised at a distance from the placental site and a portion of the fetal membranes exposed. The amnion and chorion were separated and a section of the amnion was removed and mounted on a teflon o-ring. After thorough washing with a buffered electrolytic solution[1] the specimen was inserted into the sample cell, which was filled with the same solution maintained close to 26°C.

The sample cell of 1 cm^2 cross-sectional area, was a two chamber plexiglas cylinder; the two chambers were separated by the membrane mounted on the o-ring. The platinum-platinum black electrodes were 8 mm apart, at opposite ends of the cell. The specimen presented a 1 cm^2 cross-section to transverse current flow. Field fringing was negligible with electrode separation and oscillator frequencies employed.

Equivalent parallel capacity and dissipation factor were measured with an impedance bridge (General Radio 1650-A driven by a Hewlett-Packard 200CD oscillator). Measurements were made at 23 selected frequencies between 20 and 7000 cycles/second, repeated measurements being made at 1000 cycles/second as a check for drift of impedance with time. Drift was negligible. A digital computer was used to convert the raw data into the equivalent series impedance form; the series impedance contributed by the electrodes and the electrolyte solution was subtracted during computation. (The former was measured before and after sample introduction and found to agree closely.) The data for 11 separate amnion sections were averaged and converted to the form $Z = R + jX$ at each frequency.

RESULTS

Fig. 1 shows the reactance, X, plotted against the resistance, R, at the frequencies indicated. Circles represent the experimental results; the solid curve is the best fit circular arc extrapolated to $X = 0$. The close correspondence between the experimental points and a characteristic circular arc with elevated center is strong evidence for the existence of a relaxation mechanism of the form of equation (1). The constants of equations (3) and (4) can be determined from the data shown in Fig. 1. R_0 and R_∞, the impedances in the limit of low and high frequencies, are found to

[1] The buffered electrolyte of pH 7.4 was prepared according to Robinson (7), and contained in mmoles/liter, Na+, 140; K+, 5; Ca++, 2.5; Mg++ ,1; Cl—, 144; P, 3; SO_4—, 1; and 1 gm of glucose per liter.

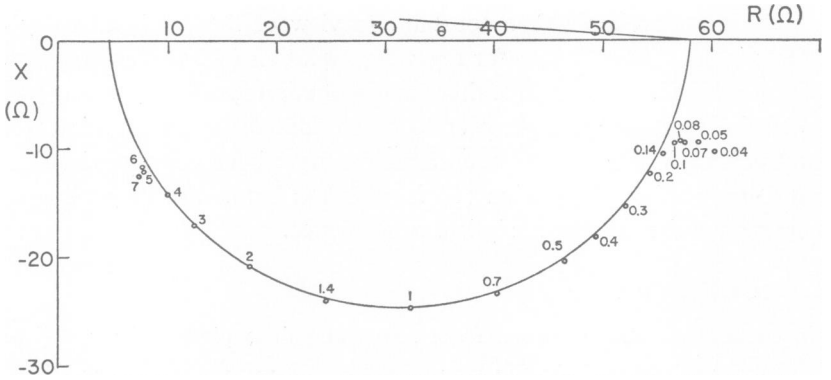

FIGURE 1 Characteristic circular arc with elevated center. Reactance plotted *vs.* resistance at each frequency (in kc/second). Circles represent observed data and the continuous line is the best fit circular arc. $\theta = \alpha\pi/2$ (see text).

be 58.0 ohms and 4.8 ohms respectively. From equation (2), the time-constant distribution parameter, α, is 0.05. From equation (4), X can be shown to reach its minimal value at $\omega\tau_0 = 1$ where $\omega = 2\pi f$ and τ_0 is the most probable τ of the time-constant distribution. From Fig. 1 and a plot of X *vs.* f, it is determined that X reaches its minimum at a frequency of 1050 cycles/second, thus $\tau_0 = 152$ microseconds. With values of R_0, R_∞, α, and τ_0 determined, equations (3) and (4) may be plotted; these relations are shown by the solid curves of Fig. 2. The experimental data (circles) are seen to coincide with the calculated values, except at the extremes of high and low frequencies.

The Cole and Cole time-constant distribution of equation (6), for the case of $\alpha = 0.05$, is presented in Fig. 3. The narrow width of the distribution is striking and will be considered later.

DISCUSSION

The electrical behavior of the amnion can be simulated by electrical circuits with frequency-independent elements. If we choose $\alpha = 0$, equation (1) precisely expresses the frequency-dependent impedance of the circuit of Fig. 4*a*, provided

$$R_1 = R_0 \tag{8}$$

$$R_2 = R_0 R_\infty/(R_0 - R_\infty) \tag{9}$$

$$C_2 = (R_0 - R_\infty)\tau/R_0^2. \tag{10}$$

Using the experimentally determined values of R_0, R_∞, and τ to evaluate equations (8) through (10) it is found that $R_1 = 58\ \Omega$, $R_2 = 5.2\ \Omega$, and $C = 2.5\ \mu$f. The effect of the approximation, $\alpha = 0$, however, is to lower the center of the circular arc to $X = 0$ and to increase the slopes of the calculated functions of Fig. 2. In order to

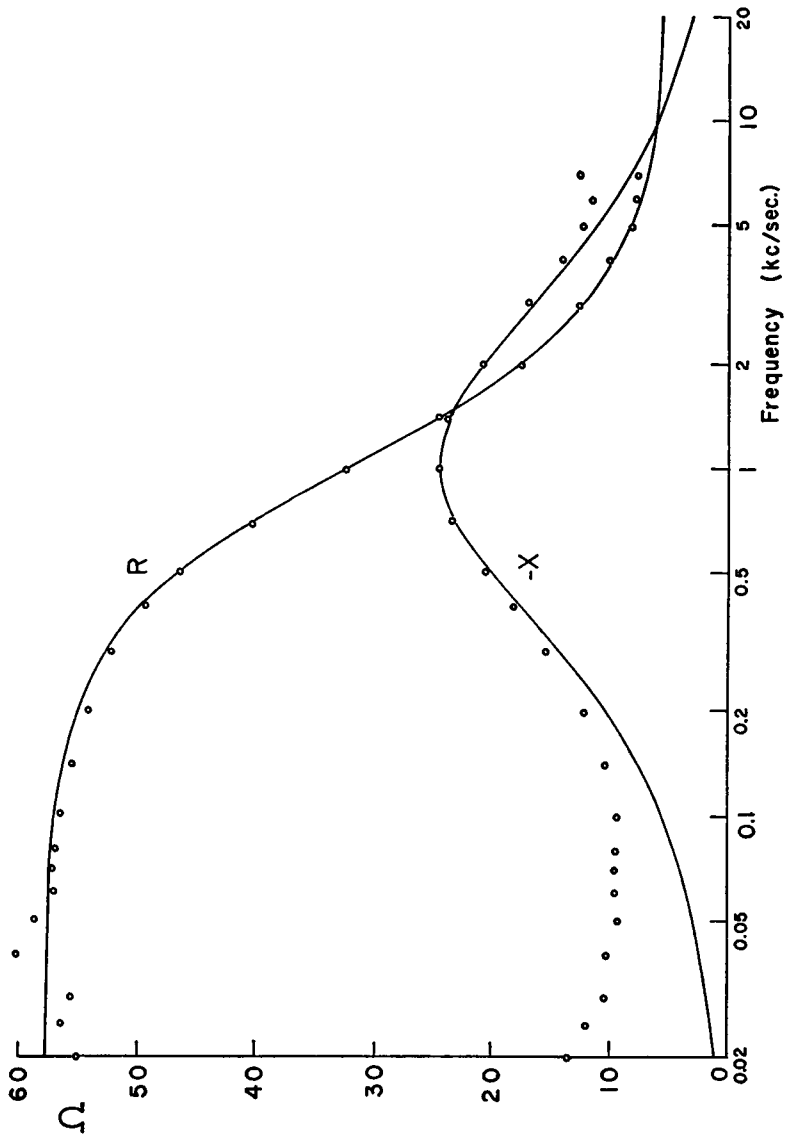

FIGURE 2 Dispersion curves. Resistance, R, and reactance, X, in ohms as functions of frequency in kc/second. Circles represent observed data and continuous lines, calculated values.

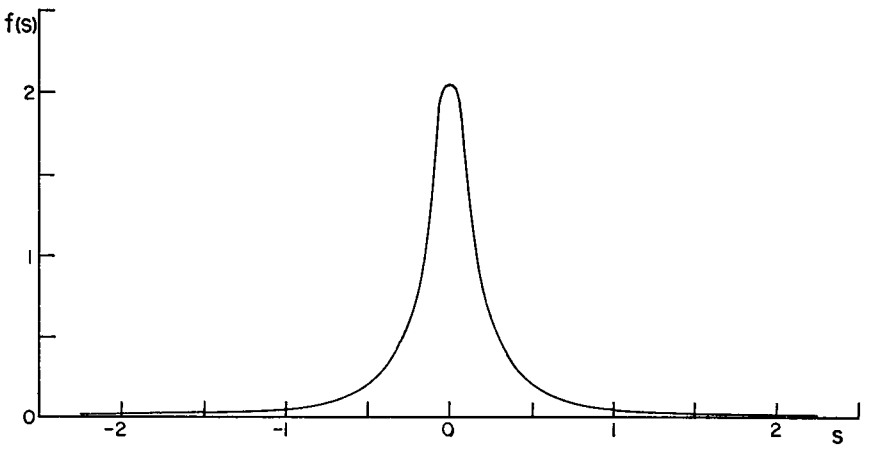

FIGURE 3 Empirical time-constant distribution function for amnion calculated from equation (12) for $\alpha = 0.05$.

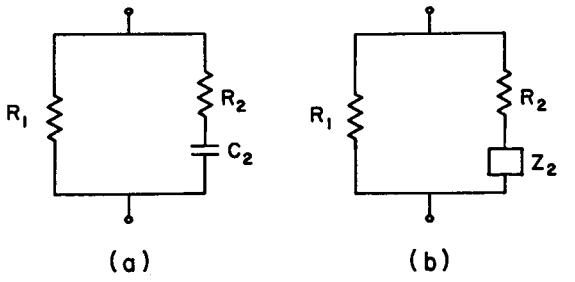

FIGURE 4 Equivalent electrical circuits of amnion. (*a*), circuit simulating single time-constant relaxation; (*b*), circuit simulating distributed time-constant relaxation.

represent the experimental findings more accurately, it is necessary to take $\alpha = 0.05$ as determined experimentally. Then the impedance of equation (1) is represented by the circuit of Fig. 4*b* provided R_1 and R_2 are given by equations (8) and (9) and

$$Z_2 = (R_1 + R_2)/(j\omega\tau_0)^{1-\alpha}. \tag{11}$$

Equation (11) can be rewritten as

$$Z_2 = \frac{R_1 + R_2}{(\omega\tau_0)^{\beta}} \exp(-j\beta\pi/2) \tag{12}$$

where $\beta = 1 - \alpha$. Thus Z_2 consists of a frequency-dependent series resistance and capacitance with constant phase angle. As ω approaches zero the dissipative or resistive part approaches infinity.

The assumption of relaxation behavior appears to be consistent with the observed results. Dispersion curves predicted analytically by equation (1) (circular arcs with

elevated centers) coincide with the experimental results very well as evidenced by Fig. 1 in which R and X are plotted against each other, frequency being the common parameter. Divergence of the experimental data from the calculated curves, however, is seen more readily when R and X are presented as functions of frequency, as in Fig. 2. The divergence at high frequencies is, in all probability, the beginning of another dispersive region; *i.e.,* Schwan's β-region (1). The possibility that this divergence was the result of experimental error introduced by stray capacitance in the neighborhood of the high frequency limit of the impedance bridge was rejected by measurements on analogous circuits of known impedance. The low frequency divergency (see Fig. 2), on the other hand, is apparently due to electrode polarization (8). If $\Delta R = R_0 - R_\infty$ and $\Delta X = X_{\min}$ then, from equation (4),

$$\Delta X = (\Delta R/2) \tan (1 - \alpha)\pi/4. \tag{13}$$

Equation (13) relates the magnitude of dispersion in X to that in R. Since $0 \leq \alpha \leq 1$ it follows that $\Delta R \geq 2\Delta X$. In view of the lack of dispersion in R it would seem improbable that this divergence represents the beginning of a subaudio dispersion.

The distribution of time constants enters the analytical formulation through equation (5); introducing the experimentally determined value of α results in the distribution of Fig. 3. The existence of this distribution implies that the relaxation mechanism springs from a polydisperse system consisting of (*a*) a geometry which is not precisely space-periodic, and (*b*) different ionic species experiencing different effective viscosities and permeabilities. Furthermore, this distribution is strikingly narrow, 87 per cent of the time constants being contained in the interval $0.67 < \tau/\tau_0 < 1.5$. This narrowness implies that, for the present experimental data, equation (5) is a rapidly converging function, which is additional justification for the use of an equation of the *form* of equation (5).

The physical mechanisms underlying the dispersive nature of amnion and other types of biological tissue are only partially understood, solution of the boundary value problem being required for more complete understanding. The following paragraphs consider the present development in relation to three other systems of biological pertinence.

Relaxation due to non-homogeneity in structure is called Maxwell-Wagner relaxation (9, 10). Beginning with a single sphere in a uniform field and then considering the effects due to the introduction of many spheres, this theory is based upon the requirement of no interactions between spheres (no cross-product terms). This is the same as requiring a small ratio of sphere diameter to sphere spacing. Thus the applicability of the theory depends upon the existence of a small packing ratio. Although the theory retains quantitative significance in some instances for packing ratios of up to 70 per cent, a solid tissue such as amnion precludes its use (cuboidal cells can be assumed spherical only for small packing ratios). Thus the relaxation observed cannot necessarily be interpreted as a transcellular phenomenon.

The next question which suggests itself is whether the dispersion observed may be attributed to extracellular mechanisms. Schwarz has extended the Maxwell-Wagner model to include counterion displacement (12). In an application of the Maxwell-Wagner theory to biological problems, it has been observed that the audio-frequency dispersion curves for suspensions of bio-matter and suspensions of solid polystyrene spheres are quite similar (11, 12). This finding implies that the dispersion springs from an extracellular phenomenon, depending upon the movement of ions surrounding the cells. This is of qualitative interest with respect to the present paper. However, the theory can not be extended to the amnion because of the requirement of a small packing ratio imposed by the Maxwell-Wagner theory.

Since biological tissue is composed of aggregates of charged components, it is appropriate to consider a further model. Schwan *et al.* (11) considered the mechanisms of electrophoresis and its application to the case of suspensions of polystyrene spheres. A colloidal particle usually carries an electric charge which accelerates the particle in the presence of an electric field. For small displacements the equation of motion is $mdv/dt + rv = qE$ where m is the mass of the particle; v, its velocity; q, the particle charge; r, the coefficient of friction; and E, the field. If the field is $E = E_0 \exp(j\omega t)$ then, under steady-state conditions, $v = v_0 \exp(j\omega t)$ and from the equation of motion,

$$v_0 = \frac{qE_0}{r} \frac{1}{1 + j\omega\tau} \tag{14}$$

where $\tau = m/r$. If n is the number of charged particles per unit volume the peak electrophoretic current density is $J_0 = nqv_0$ and thus the impedance for the present case is of the form

$$Z = 1 + j\omega\tau. \tag{15}$$

Equation (15) predicts a constant R, and an X proportional to ω (analogous to inductance), neither of which were found to exist in the present case. Therefore, the dispersion in the data is not explained on the basis of electrophoretic mechanisms.

The present paper has introduced the amniotic membrane of the guinea pig as a tissue uniquely suited for the study of biological impedance. It has been shown that the impedance characteristics of the amnion may be analyzed within the general framework of relaxation theory. Future studies will be directed toward further analysis of impedance in solid tissues and its biological significance.

SUMMARY

(*a*) The electrical impedance of amnion, over the audiofrequency range, can be represented analytically by a simple frequency-dependent function. The function is precisely of the *form* of the Debye relaxation equation.

(*b*) The observed data exhibit a broad relaxation-type dispersion centered at a frequency of 1050 cycles/second. Associated with the dispersion is a narrow dis-

tribution of time constants, the most dominant being 152 microseconds, which is due to the polydisperse nature of amniotic tissue.

(*c*) The narrowness of the time-constant distribution makes it possible to simulate amnion behavior by a simple electrical circuit of frequency-independent components.

(*d*) Due to its requirement of small packing ratio the Maxwell-Wagner treatment, successfully adapted for cell suspensions, loses its quantitative significance in the case of the tightly structured amnion. Qualitative agreement is, however, observed.

(*e*) A first order approximation of an electrophoretically controlled model predicts an electrical impedance, $Z = R + j\omega L$, containing an inductive reactance (mass controlled) and thus cannot explain the observed data.

APPENDIX

Chemical determinations were made by the following methods: *Total osmolality,* Fiske osmometer using 0.2 ml samples; *sodium and potassium,* Baird-Atomic, Inc., flame photometer, Model KY-1; *chloride,* Cotlore chloridometer automatic titrator; *magnesium,* titan yellow; *calcium,* Corinth Ca; *inorganic phosphorus,* method of Fiske; *urea nitrogen* without aeration, urease; *glucose,* enzymatic glucose oxidase; *serum total proteins,* biuret and amniotic fluid proteins, modified biuret.

In each column of Table I the first number represents the mean value; in parentheses is the range; the number of samples analyzed is in brackets. As the fetus matured, amniotic fluid, potassium, chloride, and urea increased; phosphorus and glucose decreased; total osmolality, sodium, and magnesium showed no consistent trend; protein fluctuated irregularly. Maternal and fetal plasma and urine did not show many similarities to findings in other species (13-18).

The DC potential of the amniotic cavity was measured in sixteen fetuses by a micropipette filled with amniotic fluid connected through an agar bridge to a calomel electrode. A reference electrode was connected to material blood or peritoneal cavity. The DC potential varied between 25 and 150 mv, amniotic cavity negative, with the maximum negativity usually found in the placenta. These results in the guinea pig were essentially similar to those obtained by Widdas in cats (19) and Meschia in goats (20). This potential disappeared within 20 minutes after the mother was placed in a nitrogen environment. The inside surface of isolated strips of chorion and amnion was negative compared to the outside by 20 mv or so. This potential was quite labile and disappeared rapidly particularly in the absence of a well oxygenated perfusion fluid.

The authors are very grateful to Mr. E. G. Miller for technical assistance, and to the staff of Western Data Processing Center, University of California, Los Angeles for its assistance.

Dr. Misrahy died March 7, 1964. He was a Career Research Professor under Research Grant No. NB-K6-18, 216 from the National Institute of Neurological Diseases and Blindness.

This study was supported by Research Grant No. B-3453 from the National Institute of Neurological Diseases and Blindness, United States Public Health Service.

Received for publication, April 1, 1964.

TABLE I
CHEMICAL DETERMINATIONS

	Amniotic fluid			Maternal plasma			Fetal plasma			Maternal urine			Fetal urine		
Total osmolality	*283.5	(225–304)	[34]												
mosM/kg	‡285.7	(277–300)	[7]	306	(257–345)	[25]	303	(286–330)	[13]	771	(308–1000)	[10]	330	(304–373)	[3]
Sodium	*134.9	(112.0–152.3)	[39]												
mEq/L	‡131.4	(123.3–136.0)	[7]	144.2	(111.2–163.5)	[25]	141.0	(124.2–157.1)	[13]						
Potassium	* 8.3	(3.7–15.4)	[39]												
mEq/L	‡ 19.8	(15.0–20.8)	[7]	6.0	(4.6–7.2)	[18]	5.9	(4.8–7.3)	[11]						
Chloride	*114.3	(76.9–134.6)	[39]												
mEq/L	‡137.7	(116.9–143.8)	[7]	99.5	(85.0–124.0)	[25]	94.3	(72.1–108.2)	[14]	84.3	(28.7–200.6)	[10]	85.9	(62.7–121.4)	[5]
Magnesium	* 2.3	(1.0–3.5)	[39]												
mEq/L	‡ 2.0	(1.2–3.2)	[7]	2.1	(1.1–2.7)	[22]	2.6	(2.1–2.9)	[8]						
Calcium	* 8.3	(2.9–16.0)	[38]												
mg/100 ml	‡ 4.6	(2.0–7.0)	[7]	10.2	(7.5–12.0)	[15]	10.9	(9.3–12.8)	[9]						
Inorganic phosphorus	* 2.1	(0.9–6.9)	[38]												
mg/100 ml	‡ 1.4	(0.9–1.9)	[7]	5.8	(1.1–9.0)	[21]	7.9	(6.2–8.9)	[6]						
Urea N	* 24.0	(6.4–38.5)	[37]												
mg/100 ml	‡ 30.7	(25.9–42.2)	[7]	28.1	(16.9–59.6)	[25]	26.7	(15.2–32.6)	[13]	707.1	(294.0–1800.0)	[9]	191.9	(115.0–269.5)	[5]
Glucose	* 91.0	(37.2–199.9)	[38]												
mg/100 ml	‡ 49.4	(27.5–80.0)	[7]	185.4	(84.8–248)	[20]	149.9	(93.1–238.8)	[10]						
Total proteins	* 0.092	(0.027–0.274)	[33]												
gm/100 ml	‡ 0.100	(0.052–0.169)	[7]	4.9	(3.3–6.8)	[22]	5.1	(3.9–6.8)	[13]						
DC potential		(−25 to −150 *mv*)	[16]												

*Fetal weight: 2.5 to 50 gm.
‡Fetal weight: 70 to 125 gm.

REFERENCES

1. SCHWAN, H. P., 1957, *Advances Biol. and Med. Physics*, **5**, 147.
2. DEBYE, P., 1929, Polar Molecules, New York, Dover Publications, Inc.
3. SMYTH, C. P., 1955, Dielectric Behavior and Structure, New York, McGraw-Hill Book Co., Inc.
4. COLE, K. S., and COLE, R. H., 1941, *J. Chem. Physics*, **9**, 341.
5. FUOSS, R. M., and KIRKWOOD, J. G., 1941, *J. Am. Chem. Soc.*, **63**, 385.
6. KAUZMANN, W., 1942, *Rev. Mod. Physics*, **14**, 12.
7. ROBINSON, J. R., 1949, *Biochem. J.*, **45**, 68.
8. SCHWAN, H. P., 1963, Determination of biological impedance *in* Physical Techniques in Biological Research, **6B**, (W. L. Nastuk, editor), New York, Academic Press, Inc.
9. MAXWELL, J. C., 1891, A Treatise on Electricity and Magnetism, (chapters IX and X of part II), 3rd edition, New York, Dover Publications, Inc.
10. HARTSHORN, L., 1926, *J. Inst. Elec. Engrs.*, **64**, 1152.
11. SCHWAN, H. P., SCHWARZ, G., MACZUK, J., and PAULY, H., 1962, *J. Physic. Chem.*, **66**, 2626.
12. SCHWARZ, G., 1962, *J. Physic. Chem.*, **66**, 2636.
13. ALBRITTON, E. C., 1957, Standard Values in Blood, Philadelphia, W. B. Saunders Co.
14. DAVIES, J., 1957, Gestation, (C. A. Villie, editor), New York, J. Macy, Jr., Foundation.
15. NEEDHAM, J., 1931, Chemical Embryology, London, Cambridge University Press, **1** and **2**.
16. ECONOMO-MAVROU, C., and MCCANCE, R. A., 1958, *Biochem. J.*, **68**, 573.
17. ALEXANDER, D. P., NIXON, D. A., WIDDAS, W. F., and WOHLZOPEN, F. X., 1958, *J. Physiol.*, **140**, 1.
18. MAKEPEACE, A. W., FREMONT-SMITH, F., DAILEY, M. E., and CARROLL, M. P., 1931, *Surg., Gynec. and Obst.*, **53**, 635.
19. WIDDAS, W. F., 1961, *Brit. Med. Bull.*, **17**, 107.
20. MESCHIA, G., WOLKOFF, A. S., and BARRON, D. H., 1958, *Proc. Nat. Acad. Sc.*, **44**, 483.